Open Access Journal

Journal of Sustainable Research in Engineering Vol. 8 (1) 2024, 35-49

Journal homepage: https://jsre.jkuat.ac.ke

ISSN (Online): 2409-1243

Effects of Thermal Insulation on Residual Stresses of Welded Joints

Dorcas Chege[1*] and John Kihiu[1]

[1]*Department of Mechanical Engineering, Jomo Kenyatta University of Agriculture and Technology University, P.O. Box 62000 Nairobi, Kenya.*

[*]*Corresponding Author - E-mail: dorcas.chege@jkuat.ac.ke*

Abstract: Residual stresses are generally retained in a component, such as a section of a welded pipe, assembled coupling, or angle joint for the entire service life of the component. Residual stresses contribute to tensile stresses which are partly responsible for failure of welded structures through processes such as fatigue failure, stress corrosion cracking, or corrosion fatigue. Some of the chief factors responsible for setting up residual stresses in welds include; rate of cooling, stresses already present in the parent material, type of structure and neighboring joints, heat present during welding depending on, current, electrode size, and speed in arc welding. From this research, the following conclusions were drawn. Lagging the welded pipe coupons decreased tensile residual stresses. For instance, axial tensile residual stresses on the inner surface of the pipe were lowered by 31.4 percent when 25 mm thick insulation was used. Insulating the weld caused an increase in compressive residual stresses. Axial compressive residual stresses on the outer surface of the pipe increased by 176.9 percent when 37.5 mm thick insulation was used. The aim of the research was to study ways of minimizing residual stresses in order to improve the quality of welded structures, focusing on oil pipelines. The method studied in this research was lowering the rate of cooling of welded pipe coupons by insulating them. Residual stresses in the pipe coupon were calculated using finite element simulation. ABAQUS was used to model the welding process of API 5L X65M pipe coupons. Trend-lines of stresses obtained at different cooling rates were drawn for easy comparison and conclusions made.

Keywords Welding, residual stresses, cooling rate

1. Introduction

Welding is one of the most important methods of joining metallic parts. It is widely used in today's manufacturing industries, such as nuclear, aerospace, and high-pressure vessel applications [1].

A pipeline is a system of pipes designed to carry fluids, in an energy concept this includes oil, natural gas, or other petroleum-based products over long distances, often underground [2, 3]. To transport a liquid or gas through a transmission pipeline, the fluid must be under sufficient pressure to compensate for the pressure loss due to friction and the pressure required for any elevation change [3].

Compared to transport via road and rail, pipelines are the safest means of fuel transportation, especially over long distances [4]. Still, there have been cases of pipeline failures that have resulted in fatalities and environmental damage [5, 6]. Safety is therefore a major driving force when developing pipelines. One way to ensure a high safety margin during transportation of fuel, is by development and production of line pipes with high-quality properties, especially with regard to strength, ductility, toughness, and corrosion resistance [6]. High Strength Low Alloy (HSLA) steels have since been designed to meet these requirements. Pipe materials used for transmission pipes are constructed to conform to API 5LX standards [3].

Today, pipe segments are joined by welding, but this has not always been the case, for until about 35 years ago segments were joined by screw threads or by bolted flanged joints. Welding, now considered the best method for connecting pipe segments is used even in the most demanding high-pressure and high-temperature service [7]. This is because of its ability to establish continuity at an atomic level compared to other

mechanical fastening methods. When the distance between two atoms is reduced, there develops a net force, which at some separation distance becomes zero. At this distance known as equilibrium spacing, the net potential energy is a minimum, the aggregate of atoms is stable, and the atoms are said to be bonded. Welding is able to bring large numbers of atoms comprising two separate aggregates together to the equilibrium spacing, for the atom species to bond and for the mating of these aggregates [8]. These results in a joint that is characterized by high strength, fewer leaks and fractures. There is also less fluid resistance to the flow through the pipe as no extra fittings are added [9].

For pipelines with seams, welding of pipelines takes place first in the pipe mill, where sheets made of steel are seam welded together longitudinally or spirally. The second welding of pipelines takes place in the field. This weld is normally a girth weld, i.e., a weld around the circumference [10]. The pipe welding process is governed by International Codes and Standards [11-14]. The codes are designed to protect the public by setting up the minimum acceptable level of safety for the welding processes [11]. Only high-quality pipe welds are acceptable in modern industry. For this reason, pipe welders must also be highly qualified people in their craft [15]. The codes and standards to be referred to for a given project depend on client preferences and local regulations.

Despite the recognition of welding as one of the most important fabrication processes in engineering industries, it is not free from serious setbacks like residual stresses and distortions in weldments [16].

Residual stresses are those stresses that remain in an object in the absence of external loading [6]. Residual stresses can be tensile or compressive. While tensile residual stresses are harmful, compressive residual stresses are beneficial to the welded part. The presence of tensile residual stresses makes the welded structure susceptible to fracture and fatigue. Tensile residual stresses will therefore prevent the application of full design loads to the welded structures during their service [6, 17]. Compressive residual stresses on the other hand increase both the fatigue strength and resistance to stress corrosion cracking [6, 17]. Some of the chief factors responsible for setting up residual stresses in welds include: Shape and size of the weld, rate of cooling, stresses already present in the parent material, type of structure and neighboring joints, type of joint, and method used in making the weld (tacking, back-stepping, etc.), heat present during welding depending on, current, electrode size, and speed in arc welding [18]. Though they cannot be fully eliminated, tensile residual stresses should be minimized to improve the integrity of welded structures.

2. Literature Review

2.1. Pipe Welding Techniques

There are four positions used in pipe welding. These positions are 1G, 2G, 5G, and 6G pipe welding positions [19]. The welding position of a pipe is determined by the pipe position and if the pipe is fixed or rotating. Because of gravity, the welding position affects the flow of molten filler metal. 1G pipe welding position requires the least skill while 6G welding position is the most challenging.

5G pipe welding position is similar to 1G in that the pipe is placed horizontally, with the exception that it is fixed and cannot move, as shown in Fig. 1 [19]. Laying of the weld is therefore done in a variety of different positions, including overhead, vertical up, and vertical down directions. These positions have specifications set up in ASME and API [13, 20]. This welding technique is used for welding pipelines mainly because once the pipe segments are laid they cannot be rotated during welding.

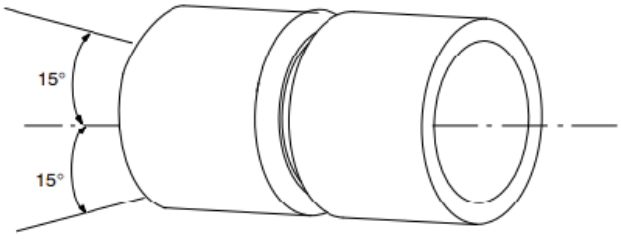

Fig. 1. 5G welding position [19]

2.2. Residual stresses in pipelines

Residual stresses are self-equilibrating stresses existing in materials or components under uniform temperature conditions. These stresses are produced if regions of a material are elastically or plastically in-homogeneously deformed in such a permanent manner that incompatibilities of the state of deformation occur. Many a time, they are inevitable and cannot be eliminated but are only minimized [6, 21].

Residual stresses encountered in pipelines may arise from a variety of sources, such as the original fabrication of the pipe sections, welding, forming, machining, grinding, handling, and even assembling of the pipeline. The final state of residual stress in any section of a pipe will arise from the differences in the amount of plastic and elastic strains created by the combined thermal-mechanical history [6].

2.3. Characteristics of Residual Stress

Since residual stresses are self-equilibrating stresses, their resultant force and the resultant moment must be zero. That means if one part of the system is altered, the rest of the system will change or adjust to maintain the equilibrium [22]. This change or adjustment results in distortion, or dimensional change, of the part involved. For example, buckling distortion is evident when compressive residual stresses generated by welding exceed the critical buckling strength of the part [23]. However, there is a positive impact to this property in that some residual stress measurement techniques use it to estimate the magnitude and direction of the residual stresses. An example of such a technique is the hole drilling method which involves drilling a small hole (i.e. small diameter and depth) normal to the surface at the point of interest and measuring the resulting local surface deformations or strains which are then converted to stresses [17, 24].

Residual stress systems are three-dimensional. From the general principles, when there is a temperature change in a body, linear expansion occurs over the total volumetric body [22]. These time- and position-dependent thermal and transformation strains are what cause elastic or elastic-plastic stress fields as well as related local and global deformations [25]. In this regard, a full description of residual stresses in a shaft can be thought of in the longitudinal, circumferential, and radial directions. In a flat surface, such as a sheet or plate, they are in the longitudinal, transverse, and thickness directions [22].

Residual stress systems are described in terms of tensile and compressive stresses. This is a corollary to Newton's third law of motion: Every force must have an equal and opposite reactive or balancing force. The effect of these stresses is different, i.e., while tensile residual stresses are generally detrimental, compressive residual stress can markedly improve performance [6, 22]. For instance, it is well established that a crack will not propagate into a layer under compression [26].

Compressive residual stresses can be used to neutralize, or counteract, potentially damaging tensile applied stresses [22]. In many cases, the functional behavior of components is determined by the mechanical and structural properties of their near-surface regions [8]. For instance, for best resistance to fatigue fracture, the surface areas should have compressive residual stresses in directions that are perpendicular to the expected fatigue-crack direction, provided that the maximum applied tensile stresses are expected to be at the surface. Similarly, tensile residual stresses on or near the surface of most parts should be avoided because they add to the tensile stresses developed while in service and may cause premature failure [6].

2.4. Influence of Residual Stress on Performance

Because of their self-equilibrating character, the presence of residual stresses may not be readily apparent and so they may be overlooked or ignored during engineering design. They remain in equilibrium in the body indefinitely after creation by thermal-mechanical processes that cause non-uniform plastic deformation.

When considering the structural integrity or mechanical performance of a component, residual stresses act in addition to applied loads (stresses). Therefore, residual stresses should be treated in the same way as applied stresses when assessing a component's fitness for purpose. In the case of pipelines, stresses from pressurization, suspended loads, vibration during operation from pumping cycles, earthquakes, soil settling, and so on would be directly summed with existing residual stresses in the pipe [6, 26].

Pipelines are subject to failure in service primarily by fatigue, stress corrosion cracking (SCC), or corrosion fatigue (CF), all of which require a net tensile stress at the surface for initiation [6].

Stress corrosion cracking (SCC) refers to the propagation of cracks under a static tensile load in the presence of a chemically active environment to which the material is susceptible. Since both chemical and mechanical factors are involved, only materials exposed to particular corrosive environments while under mechanical stress are susceptible to SCC. The residual stresses left behind by welding are often sufficient to initiate SCC in areas where it would not otherwise occur due to the lack of a sufficient mechanical driving force [6, 27].

Fatigue failure is by cyclic loading to stress levels above the endurance limit of the material. Cracks initiate at the surface or from some internal flaw, such as an inclusion in the metal. Fatigue is classified as either low cycle fatigue (LCF) or high cycle fatigue (HCF), depending upon the stress amplitude level and number of cycles to failure. High-cycle fatigue requires more than 10^4 cycles to fail. It often occurs in cases where stress is low and primarily elastic. Low cycle fatigue is characterized by repeated plastic deformation in each cycle and therefore, the number of cycles to failure is low. HCF occurs more commonly in pipelines, under essentially elastic cyclic loading, and failures occur only after 1 million or more cycles. Welding residual stresses have a dominant influence on the mean stress and fatigue performance in pipelines [28, 29].

Cracking is one of the major defects of welding. In

general, cracking may occur years after the weld is completed or during manufacturing of the weldment. It can be a result of rapid cooling, restraint, residual stresses, contamination from the atmosphere, etc. [30, 31]. Cracking that occurs during the solidification of the weld metal is known as solidification cracking or hot cracking [31]. Unlike hot cracking, cold cracks appear hours or even days, after the weld cools. Broadly speaking, cold cracking occurs as the result of residual stresses from the base material restraining the weld, along with the presence of diffusible hydrogen. Cold cracking is particularly prevalent in thick materials, as they tend to create areas of high restraint and can serve as a heat sink that leads to fast cooling rates. Such rapid cooling causes the formation of martensite. While very hard, martensite is also very brittle and lacks ductility. Martensite provides a location for diffusible hydrogen to coalesce, which in turn creates residual stresses. Once these residual stresses reach a critical level, cold cracking occurs [30].

Corrosion fatigue is the combination of mechanical fatigue-generated cracks that are further propagated in a chemically aggressive environment by SCC. The presence of residual stresses adds to the mean stress, and can either exacerbate or mitigate SCC. The corrosion debit during fatigue in pipeline steels requires tension exceeding a threshold level, and is mitigated by reducing tensile or introducing compressive residual stress [29].

2.5. Gaps for Study

Though it is widely accepted that tensile residual stresses from any origin render the pipeline more likely to fail, their effects are often ignored. For instance, during welding qualification, no attention is given to residual stresses. Some of the pipeline design codes widely used in the manufacturing of pipelines include DNVGL-ST-F101, PD 8010, ASME B31.8, API RP1111, ISO 13623, and EN 14161. Each of these codes has a range of applications and limitations, e.g., DNVGL-ST-F101 and API RP1111 apply to the design of offshore pipelines only. In general, none of these pipeline design codes addresses residual stress explicitly at the design stage [32]. Since the codes are adhered to during pipeline welding, it implies that residual stresses are disregarded in the pipeline installation process. However, with the recent understanding of the effects of residual stresses, it is evident that these stresses should be put into consideration to improve the quality of welded structures. Furthermore, as the future of engineering is gearing towards performance-based design (PBD), factors like residual stress can be the difference between a successful and a failed performance prediction.

In this regard, studies on various techniques for reducing residual stresses during installation are key to improving the integrity of welded structures.

In this study control of welding parameters, i.e., cooling rate as a method of reducing residual stresses during pipeline installation was studied.

2.6. Welding Residual Stress Simulation: Governing Equation

Residual stresses were determined using ABAQUS simulation software. To give a full description of the problem a governing equation is normally combined with initial and boundary conditions. The governing equation for the transient non-linear heat transfer analysis is the Fourier heat conduction, equation 1 [33].

$$C\rho\frac{\Delta T}{\Delta t} = \frac{\partial^2 T}{\partial x^2}k_x + \frac{\partial^2 T}{\partial y^2}k_y + \frac{\partial^2 T}{\partial z^2}k_Z + Q \qquad (1)$$

Where k_x, k_y, and k_z are thermal conductivities in the x, y, and z directions respectively, T is the current temperature, Q is the heat generation, ρ is the density, C is the specific heat capacity and t is the time, respectively.

The solution to Equation 1 requires initial and boundary conditions. Both the initial temperature of the specimen at time zero or the start of the welding process and the ambient temperature, have a significant role during the heating and cooling phases [33]. The initial conditions describe the distribution of temperature at all points in the interior of the domain. The initial condition is stated as in the equation 2 [33].

$$T(x, y, z, 0) = T_0 \qquad (2)$$

The boundary conditions mostly considered are surface convection and surface radiation. The surface convection equation taken into consideration follows Newton's law of cooling, which is given by equation 3 [34].

$$q_{conv} = h_{conv}(T - T_0) \qquad (3)$$

h_{conv} is the heat transfer or film coefficient and T_0 is the sink temperature. According to Stefan Boltzmann's law, heat loss by radiation is given by equation 4 [34].

$$q_{rad} = \varepsilon.\sigma.((T - T_z)^4 - (T_0 - T_Z)^4) \qquad (4)$$

ε is the emissivity constant, σ is the Stefan-Boltzmann constant, and T_z is the absolute zero on the actual temperature scale considered. A convenient formulation of the boundary value problem of heat conduction involves the radiation loss calculated using an

equivalent film coefficient given by equation 5. [34, 35]

$$q_{rad} = h_{rad}(T - T_0) \qquad (5)$$

h_{rad} is the equivalent film coefficient. With the boundary condition, the complete solution of the given problem can be written as shown in equation 6.

$$k\Delta T - q + h(T - T_0) + \sigma\varepsilon(T^4 - T_0{}^4) = 0 \qquad (6)$$

2.7. Transient Thermal Analysis

Modeling of the heat input of a welding process can be achieved using three approaches: a static heat source with prescribed temperature, a static heat source with volumetric flux, and a moving heat source with volumetric flux, in order of increasing complexity and accuracy [36]. The weld pass heat input per unit run length Q can be calculated from welding process parameters as shown in equation 7 [36].

$$Q = \eta IU/v \qquad (7)$$

Where I is the current, U is voltage, η is the electrical heat input efficiency per welding process, and v is weld travel speed. When a 2D approximation is used, e.g., rotational symmetry for simulating pipe girth welding, the assumed conditions in the model resemble those corresponding to a simultaneous deposition of the weld pass along the entire weld length [36].

A typical heat source model for arc welding processes such as MMAW, SAW, and TIG is illustrated in Fig. 2.

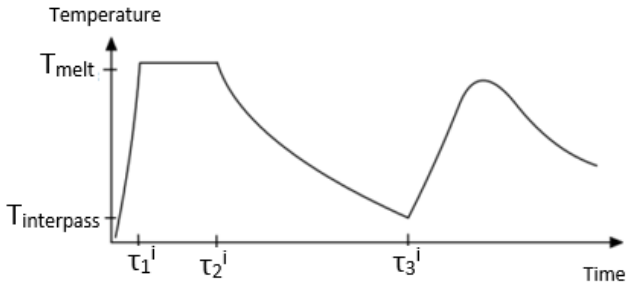

Fig. 2. Transient-temperature vs. time for a newly deposited weld pass [37]

Fig. 2 shows the temperature in the centre of a newly added weld bead. The temperature is rapidly rising to the melting temperature T_{melt} and the filler material holds that temperature under the period τ_2^i, before it starts to cool down and solidify, since the weld pool is moving on. For these welding processes, the dominating part of the molten material is the newly added filler material, and the majority of heat (Q) is consumed by the new filler material. The time τ_1^i is short compared to τ_2^i. The material continues to cool down and has the temperature $T_{intpass}$ at the instant τ_3^i when the next adjacent weld pass is made [37].

2.8. Thermo-elastic-plastic Mechanical Analysis

Once the temperature history is generated as described in the latter sections, stresses and strains are calculated by performing a thermo-elastic-plastic analysis. Small strain theory is normally used. The analysis follows the given temperature history on a pass-per-pass basis until all weld passes are simulated. The mechanical properties are temperature-dependent. Incremental plasticity is used with the von Mises yield criterion and associated flow rule. The material hardening law is assumed to be isotropic hardening. From recent comparisons, measured weld residual stress fields indicate that through-thickness stress profiles are better captured using an isotropic hardening model [28, 38]. If detailed cyclic stress-strain material properties are available, then a mixed isotropic-kinematic hardening model could be used (an expanding and translating yield surface). The multi-pass weld is modeled by activating the elements belonging to the current pass at a proper time, consistent with the transient heat flow simulation procedure.

Boundary conditions resembling the fixing conditions used during the welding are applied to the model. Any post-weld heat treatment and mechanical loading that may redistribute the residual stress field should also be modelled [36, 37].

3. Methodology

The aim of the research was to study ways of minimizing residual stresses to improve the quality of welded structures. The method studied in this research was lowering the rate of cooling of welded pipe coupons by insulating them. Residual stresses in the pipe coupons were calculated using finite element simulation.

Welding simulation was done by coupling thermal and stress (structural) analysis. Thermal analysis was performed first and then the temperatures calculated in this thermal analysis were applied during the structural analysis. With this method, the structural properties did not influence the thermal results. ABAQUS was used to model the welding process. The actual welding process was then done, and temperature history at certain locations was measured using thermocouples. The temperature history data was used for verification during thermal analysis.

3.1. Description of the Welded Pipe

The material of the pipe used for this research is API 5L X65M pipeline steel. This is a High Strength Low Alloy

(HSLA) steel that is common for gas and petroleum pipelines. The Chemical composition of the parent material is shown in Table 1.

Table 1. Chemical composition of the base metal [27]

Mass fraction, based upon heat and product analyses									Carbon equivalent% maximum
C[a]	Si	Mn[a]	P	S	V	Nb	Ti	other[d]	CE_{pcm}
0.12	0.45	1.6	0.025	0.015	b	b	b	c	0.23

[a]For each reduction of 0.01% below the specified maximum for carbon, an increase of 0.05% above the specified maximum for manganese is permissible up to a maximum of 1.75%.
[b]The sum of the niobium, vanadium, and titanium concentrations shall be 0.15%
[c]Unless otherwise agreed, 0.5% maximum for copper, 0.3% maximum for nickel, 0.3% maximum for chromium and 0.15% maximum for molybdenum
[d]0.004% maximum for boron

3.2. Specimen Preparation: Beveling

To prepare the specimens, the pipe was cut into coupons each 6 cm long after which they were beveled and ground to provide the V groove, Fig. 3. A single-V groove with a bevel angle of 30 degrees was chosen since this was the weld configuration used for the newly constructed Mombasa-Nairobi pipeline. The dimensions of the pipe coupons used in this study were: 60 mm long with an inner diameter (d) of 508 mm and a wall thickness (t) of 9.0 mm.

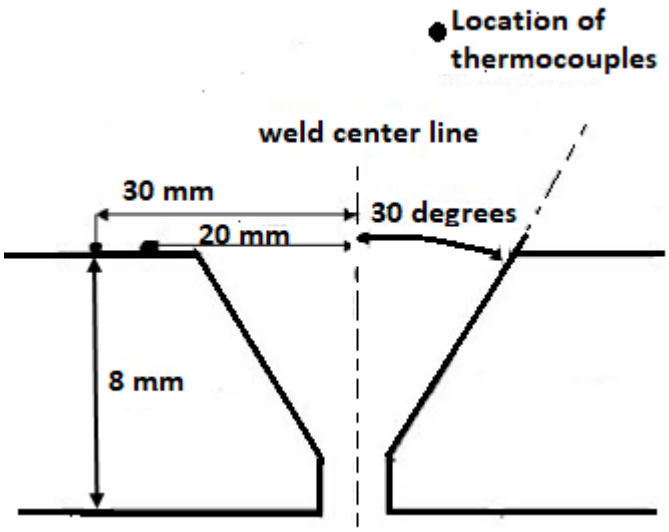

Fig. 3. Schematic diagram of the weld.

Welding was done using the MMAW welding process. This welding technique was chosen based on the availability of the welding equipment needed.

3.3. Welding Procedure

Tack welds were first created. To achieve this E6010 electrodes were used. These electrodes were used because they were the same electrodes used to make the root pass. The current was set to 60 Amperes, and spacers 2.5 mm thick were placed between the pipe coupons. Grinding was done to remove the slag formed due to the welding process. To correct any incorrectly done tack weld a cutting disk was used.

Laying of root and hot-pass beads was done using DCSP. Filler and capping were done using reverse polarity for enhanced deposition. Different polarities were obtained by connecting the welding electrode either on the negative terminal (DCSP) or the positive terminal (DCEP) of the same MMAW machine. 5G welding position was used to weld the pipe coupons.

During welding, the pipe coupons were fixed horizontally, no clamping was employed. A fixture was welded onto the welding booth which was used to hold the pipe coupons in position. The coupons were welded by two welders using mechanically controlled welding torches. Welds were laid simultaneously on both sides. One of the welders deposited the weld along the pipe circumference covering 180 degrees of the weld joint from the 12 o'clock (weld start) to the 6 o'clock (weld stop) position. The second welder deposited the weld beads also covering an angle of 180 degrees from the 6 o'clock mark to the 12 o'clock mark for the vertical-down welding direction. This was reversed in the case of vertical-up welding direction. The weld passes done were root pass, a hot pass, fill, and capping to fill the weld groove. All the welds were laid using MMAW technique. The welding parameters are shown in Table 2.

Table 2. Welding parameters used during the welding process.

Pass	Current(A)	Voltage(V)	Welding speed(mm/min)

Root pass	55-65	35-55	14.508
Hot pass	70	35-40	66.841
Fill pass	100-105	20-35	23.018
Capping pass	100-105	20-35	23.152

3.4. Temperature Recording

Welding thermal cycles were recorded using Dataq data logger 4-channel input modules. WINDAQ data acquisition software was used to record waveforms directly and continuously to the PC while monitoring a real-time display of the waveforms on-screen. The data was then exported from the WINDAQ waveform browser to Excel software for further analysis.

3.5. Thermocouple Installation on The Pipe

To measure the transient change in temperature history during the welding process, type R thermocouples were installed onto the outer surfaces of the pipes at 10 and 2 o'clock locations in terms of the 5G welding position (horizontal fixed). The location of the thermocouple was 20 mm and 30 mm away from the weld-center line, as shown in Fig. 3.

3.6. Cooling Rate

In this research, the welded pipe coupons were covered with a polycrystalline fiber blanket immediately after welding and allowed to cool to room temperature, as shown in Fig. 4. No preheating was done.

Fig. 4. Pipe coupons covered with a 12.5 mm thick insulator.

3.7. Finite Element Modeling of Welding Residual Stress

3.7.1. Element Type and Mesh Design

In this study, the first-order 4-node linear axisymmetric heat transfer quadrilateral elements (DCAX4) provided by Abaqus software were employed for thermal analysis. For structural analysis, CAX8R elements were used. The CAX8R is a second-order 8-node bi-quadratic element with reduced integration. The elements were chosen based on their ability to provide better accuracy when performing coupled thermal–stress analysis on axisymmetric models [39- 41].

To create proper elements, partitioning of the model was done. There was a high degree of mesh refinement at the weld zone to capture the steep thermal and stress gradient during welding. Mesh sensitivity tests were done by applying the heat flux and heat loss boundary conditions to models with different mesh sizes. Temperatures from the simulations were then compared to experimental results from thermocouple measurements to obtain the optimum mesh size.

For the insulation material, the element type used was also the linear quadrilateral elements of type DCAX4. An even distribution was used during meshing of the insulations of different thicknesses as compared to the pipe models in which a denser mesh was created near the welded zone.

3.7.2. Material Properties

Material property data used for this study was collected from literature surveys [42]. For both parent and weld metals, the same values of material properties were applied. The mass density and the Poisson's ratio of the materials were 7850 kg/m^3 and 0.3 respectively.

The insulating material was made of a polycrystalline fiber blanket. Its material properties were as follows, thermal conductivity was 0.16 W/mm/K, density was 128 kg/m^3 and specific heat capacity was 1170 J/[kg. K].

3.7.3. Heat Source Modeling

The first stage of the simulation is thermal analysis. The welding process was primarily simulated by assigning distributed heat flux (DFLUX) to individual elements, in the units, power/unit volume. This is a triangular function of heat per unit volume against time. The distributed heat flux (DFLUX) was calculated using equation 7 [43, 44].

3.7.4. Modeling of Thermal Cycles

The multipass weld was modeled by activating the elements belonging to the current pass at a proper time, consistent with the transient heat flow simulation procedure. To adequately represent a real-life welding process an inter-pass temperature was incorporated between the heating cycles. Weld zone materials in the multipass welding process experienced a sequence of heating and cooling in a certain time period, which was

modeled in the STEP module. In each weld pass, heating and cooling steps were created with assigned distributed heat flux calculated using equation 7 and the cooling time used being the time recorded using thermocouples during the welding process.

The addition of filler material was modeled by de-activating and re-activating the elements that represented each pass. All the elements in the weld region were deactivated before initiating the first heating step. The deposition of the weld metal was achieved by activating the elements defined for each pass, which were isolated from the previous passes.

3.7.5. Modeling of Thermal Boundary Conditions

This research took into consideration both radiation and convection as thermal boundary conditions applied during the welding and cooling cycles. Heat loss by convection was simulated by applying film conditions while for radiation, surface radiation was used. Application of thermal boundary conditions was done to the outer edges of the construct. Thermal boundary conditions were applied to all boundaries of the pipe as well as the new boundaries created by each new pass.

3.7.6. Modeling of Heat Transfer for the Insulated Pipe

During the actual welding process, the pipe was first welded and immediately after welding it was covered with a polycrystalline fiber blanket to control the cooling rate. To model this a transverse section of the insulation was created in the part module and was later assembled with the pipe in the assembly module. The insulation was deactivated at the beginning of the simulation using model change provided in Abaqus and later reactivated immediately after the last layer of weld was laid.

The pipe was then allowed to cool to room temperature. A tie contact was created between the insulation and the pipe, as shown in Fig. 5. This was done to ensure that the pipe and insulating surfaces formed and maintained contact for the entire duration of the simulation. An outer surface of the insulating material was created, and heat loss by convection was initiated during the last step of the simulation by creating a surface film condition in the interaction module.

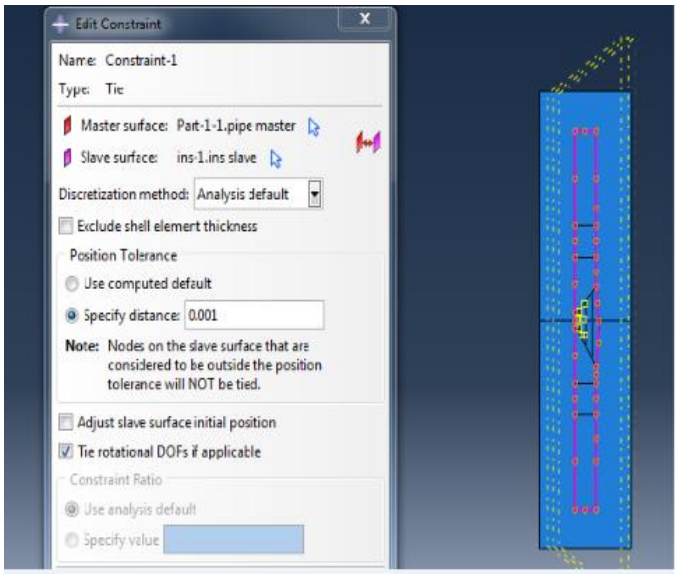

Fig. 5. Tie contact between the insulation material and the welded axisymmetrical pipe

3.7.7. Structural Modeling

A mechanical model was created based on the previously established thermal model. During structural modeling, a new model was created in the same model database and the parts, instances, materials, and sections were copied using the model copy objects option so that they were identical to those of the thermal model. Some changes were however made in terms of step type, load, and boundary conditions. The elements were changed to CAX8R. No further changes were made to the mesh. The number of steps created and each step's time were in line with those of the thermal model. The approach of deactivation/activation of the weld beads was also employed to simulate weld depositions. However, the step type was changed from heat transfer (in the thermal model) to general static.

The temperature that was calculated in the thermal analysis, was applied to the structural analysis using a predefined field. Abaqus also requires the selection of the step at which to start reading results and also the step at which to stop reading results. 0 was input at end increment this ensured that results from thermal analysis were read up to and including the last increment. Since the same mesh was used for the thermal and structural analysis, the mesh compatibility was set to 'compatible'.

The predefined field was modified in the cooling step so that it referred to the cooling step in the thermal analysis. Abaqus was now able to obtain all the information it needed to prescribe the temperature from thermal analysis to structural analysis.

For the mechanical model, there was no external load applied to the pipe, the stresses/strains were generated from thermal history.

4. Results and Discussion

4.1. Insulation

In this study, cooling was slowed using an insulator. Fig. 6 shows the time it took the pipe coupons to cool to room temperature from the time the last weld pass was laid, under the different cooling conditions.

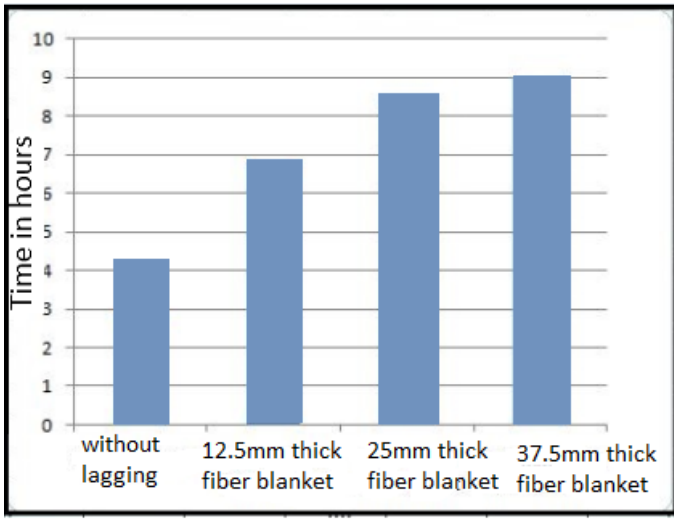

Fig. 6. Time to cool to room temperature

From Fig. 6, it can be observed that the welded pipe coupons took longer to cool when they were covered with insulators compared to when the pipe was allowed to cool in air. This is in line with the function of insulators. Thermal insulators are designed to slow the flow of heat between objects in thermal contact [45]. The type of insulator used in this research was a polycrystalline fiber blanket whose properties are discussed in the methodology chapter. When the 12.5 mm thick insulation blanket was placed on the welded pipe coupons, the time it took to cool to room temperature increased by 60.1 percent, compared to the one that cooled in air. With the use of a 25 mm thick fiber blanket, the increase was 97.21 percent. For the 37.5 mm fiber blanket, the increase was 108.8 percent. In welding the more control one has over heat, the more one can be able to counteract stress, and the less chance there is for weld distortion and cracking, especially in highly restrained joints. The slower the cooling rate, the more the reduction of shrinkage stresses. A slow cooling rate also provides more time for hydrogen to dissipate, reducing the chance of under-bead cracking [30, 31].

4.2. Thermal Analysis Results and Discussion

During multipass welding, the welded pipe was subjected to a series of localized heating and cooling cycles. It was therefore important for verification purposes that the temperature cycles got recorded to help know the exact values of temperatures on the welded structures. To help achieve this, thermocouples were placed at distances of 20 mm and 30 mm away from the weld center. Figures 7 - 14 show a comparison between the measured and simulated thermal cycles, i.e., the transient temperatures of heating and cooling cycles at specific locations on the specimen where thermocouples were installed.

4.2.1. Model Without Insulation

Fig. 7 shows the temperature history of a node located 20 mm from the weld center-line, for the sample that cooled in air.

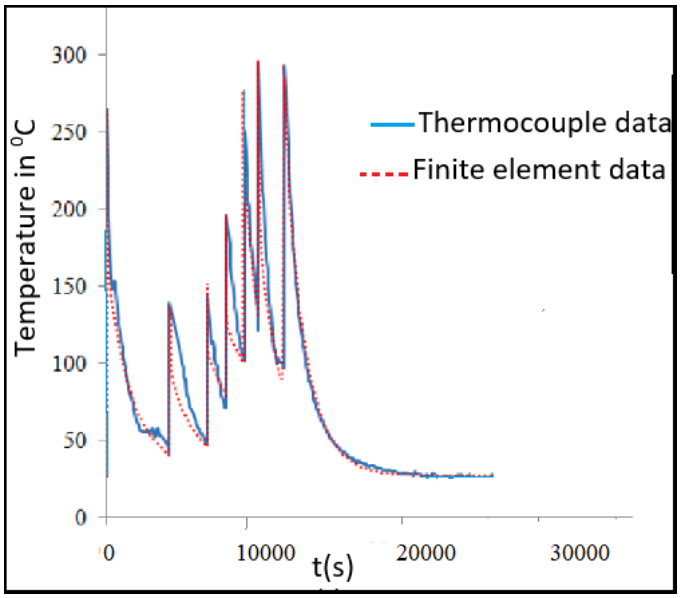

Fig. 7. Temperature history at 20 mm thermocouple location for the model without insulation.

Fig. 8 shows the temperature history of a node located 30 mm from the weld center line.

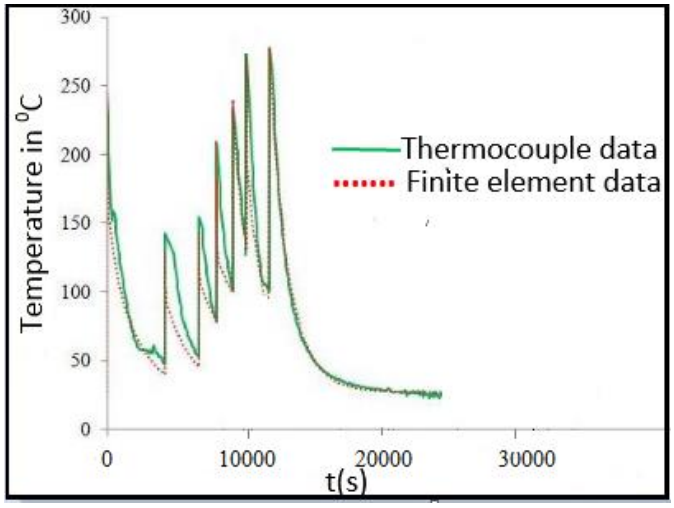

Fig. 8. Temperature history at 30 mm thermocouple location for the model without insulation

4.2.2. Model with 12.5 mm Insulation

Fig. 9 shows the temperature history of a node located 20 mm from the weld center-line, for the sample that was covered with a 12.5 mm thick insulator.

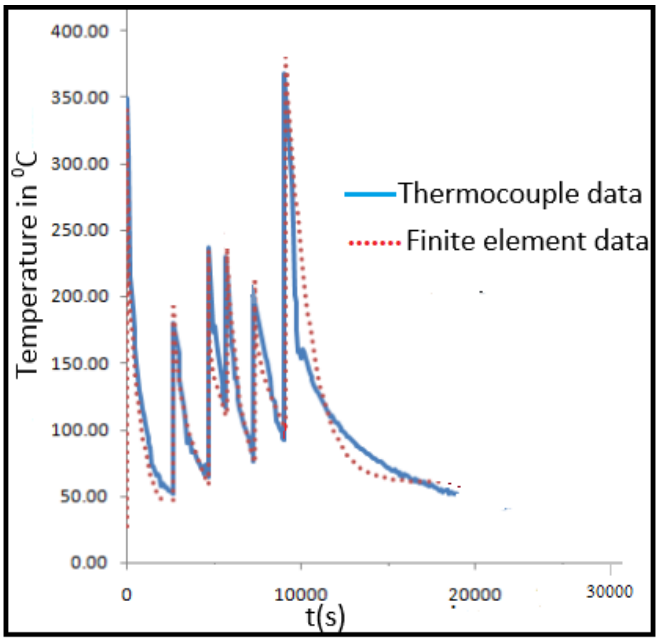

Fig. 9. Temperature history at 20 mm thermocouple location for the model with 12.5 mm insulation.

Fig. 10 shows the temperature history of a node located 30 mm from the weld center-line, for the sample that was covered by a 12.5 mm insulator.

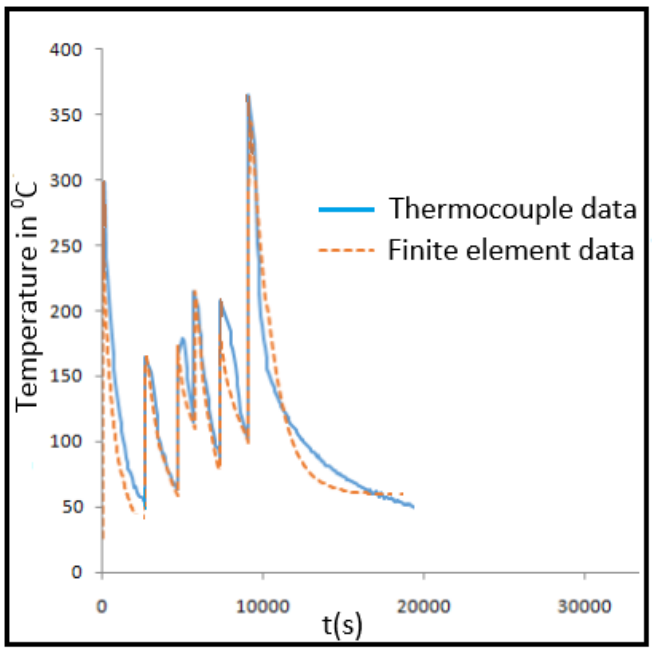

Fig. 10. Temperature history at 30 mm thermocouple location for the model with 12.5 mm insulation.

4.2.3.Model with 25 mm Insulation

Fig. 11 shows the temperature history of a node located 20 mm from the weld center line.

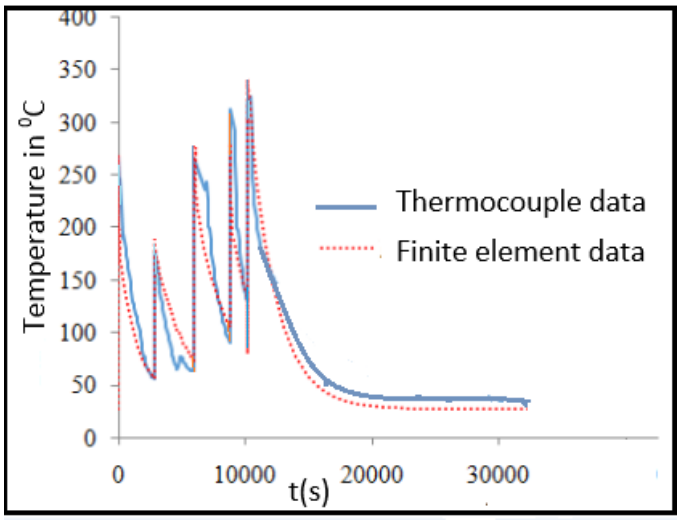

Fig. 11. Temperature history at 20 mm thermocouple location for the model with 25 mm insulation

Fig. 12 shows the temperature history of a node located 30 mm from the weld center-line, for the model covered with 25 mm thick insulation.

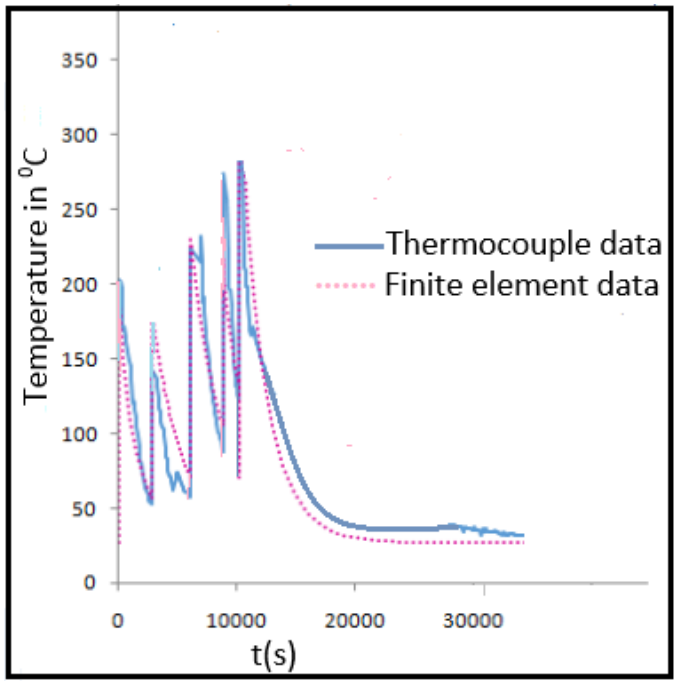

Fig. 12. Temperature history at 30 mm thermocouple location for the model with 25 mm insulation.

4.2.4.Model with 37.5 mm Insulation

Fig. 13 shows the temperature history of a node located 20 mm from the weld center line.

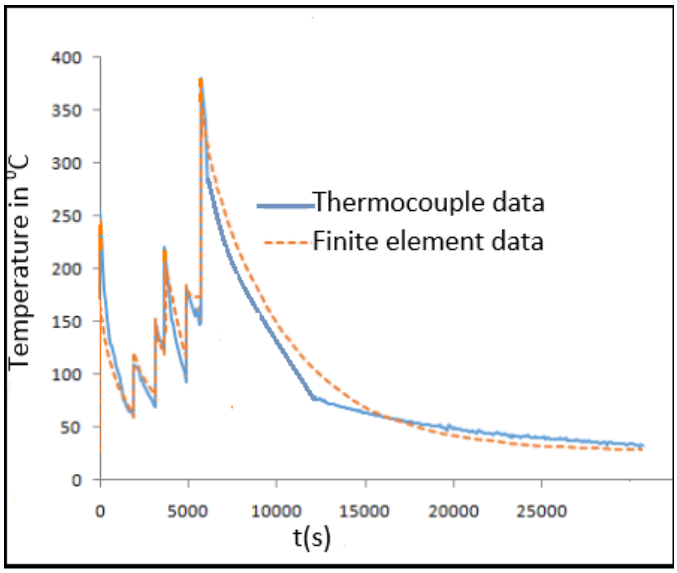

Fig. 13. Temperature history at 20 mm thermocouple location for the model with 37.5 mm insulation.

Fig. 14 shows the temperature history of a node located 30 mm from the weld center line.

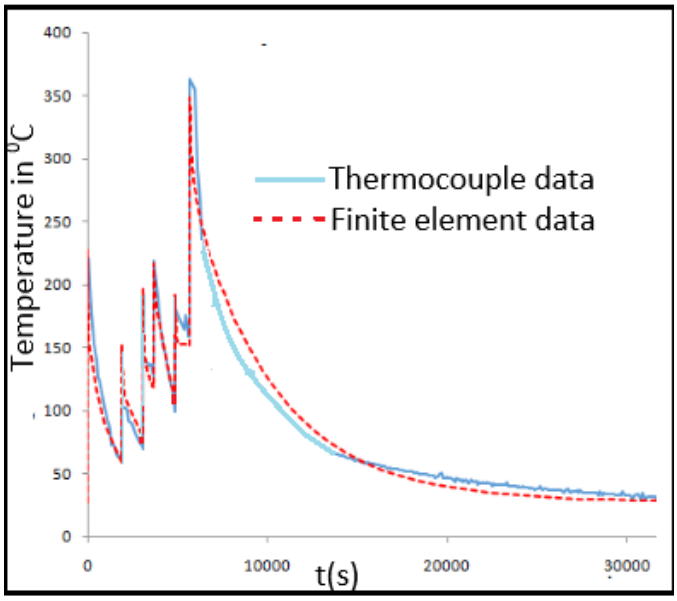

Fig. 14. Temperature history at 30 mm thermocouple location for the model with 37.5 mm insulation.

From the graphs in Figures 7-14, it can be observed that the pipe coupons underwent repeated thermal cycles throughout the welding process. Temperature histories give an insight into how temperature varies with time at chosen locations throughout the welding process. The ambient temperature was set as 27°C. Ambient temperature is set as the temperature of the model before the heat source is applied in cases where no pre-heating is done. As the heat source is applied there is a rapid increase in temperature with the maximum temperature being recorded once the heat source reaches the point where the thermocouples are located. As the heat source moves away from the thermocouple location the temperature begins to drop to an interpass temperature. Temperature begins to rise again as the welding torch begins to approach the thermocouples. In the graph, this can be seen as temperature rising to a peak value and then dropping to an interpass temperature before rising again. In the case of multipass welding, as was done in this research, these thermal cycles are repeated until all the passes are completed. Finally, the joint was allowed to cool in air to room temperature. In some cases, insulation was applied while in others cooling was done without insulation as indicated in Figures 7-14. The thermal histories were used for verification during thermal analysis in finite element analysis.

The peak temperatures are below the melting point of the base metal for both the simulated and the experimented results. This is because in welding, melting only occurs in the fusion zone area. Each peak temperature represents a weld pass.

In all the specimens that cooled under an insulator, there was a deviation between the finite element and the experimental data in the last cycle where the specimen cooled to room temperature. This can be attributed to the fact that the thermocouples were disturbed while installing the insulator. This was not the case for the pipe coupon that cooled in air it was therefore used to determine the cooling conditions required during simulation.

4.3. Residual Stress Results

The following sections contain the structural analysis results for the four pipe coupons analyzed in this work. Results are presented as stress profiles where the stresses along a path on the inner and outer surfaces of the models have been plotted against the distance along the path. The stresses on the surfaces of the pipes are of particular importance as they can initiate harmful processes such as SCC, corrosion fatigue, etc. The results are presented in a case-by-case manner.

4.3.1. Residual Axial Stresses

A graphical comparison of the simulated axial residual stresses is shown in Figures 15-17. To be able to make adequate conclusions, cases 2 (12.5 mm insulator), 3 (25 mm thick insulator), and 4 (37.5mm thick insulator) were simulated twice. The first simulation was done without insulating the models. In the second simulation, the models were insulated and allowed to cool to room temperature. For these cases, thermal cycles and time to cool to room temperature were verified as shown in Figures 9-14. To cool to room temperature, the cooling conditions verified in Figures 7 and 8 were used.

The graphs were drawn using polynomial trend lines of order 6 to show the general pattern of data over time as compared to drawing the residual stress using the fast-changing node-by-node residual stress data.

4.3.1.1 Axial Stress Distribution for the Inner Pipe Surfaces

Axial stress distribution on the inner pipe surface is indicated in Figures 15-17.

Figures 15-17 show the residual stress distribution for the pipe coupons that were covered with insulators of thicknesses 12.5 mm, 25 mm, and 37.5 mm respectively. Generally, it can be observed that the stresses along the weld center line (at x=0 mm) are tensile and become compressive in nature as one moves away from the weld center line for all the graphs. These findings have also been observed by other researchers [46, 47].

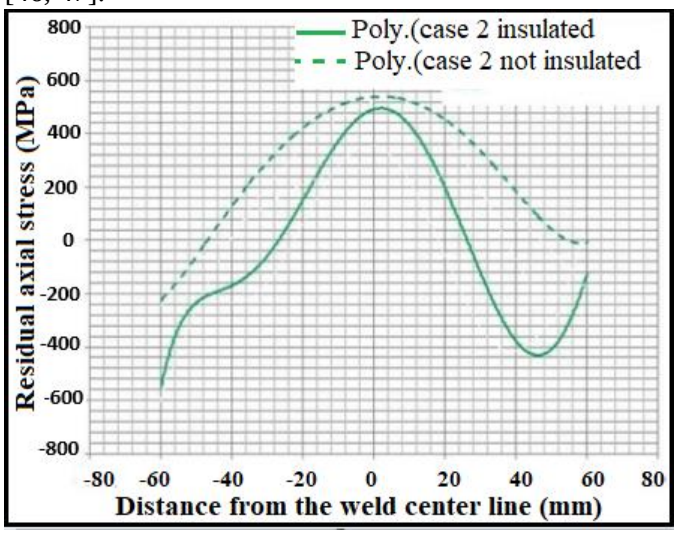

Fig. 15. Simulated axial stress distribution for the inner pipe surfaces for case 2.

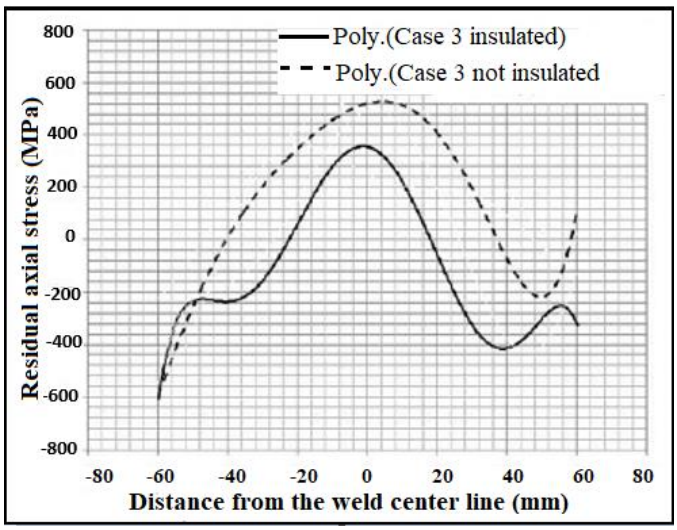

Fig. 16. Simulated axial stress distribution for the inner pipe surfaces for case 3.

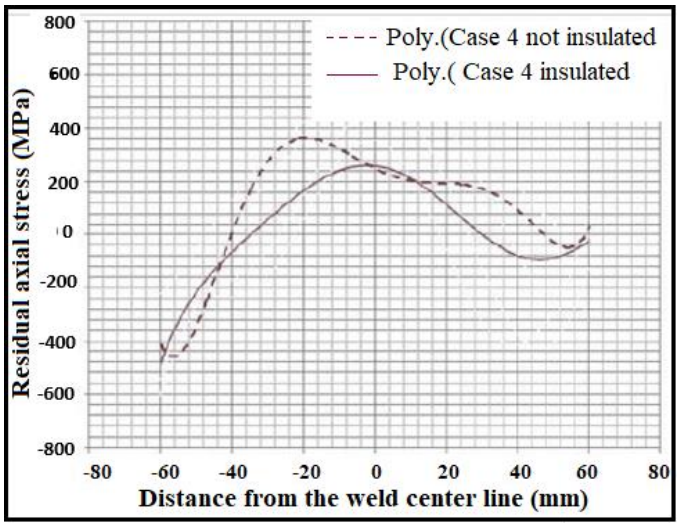

Fig. 17. Simulated axial stress distribution for the inner pipe surfaces for case 4.

This is because of the temperature gradient created by localized heating during the welding process. The temperature gradient increases with an increase in distance from the weld zone. During the welding process, the weld zone is heated to temperatures above the melting point of the base metal. The material in the weld zone expands. However, the expansion is restrained by the surrounding colder area. On cooling, the molten area cools and contracts since the contraction is also restrained, tensile residual stress is created in the longitudinal direction. Residual stresses are self-equilibrating in nature, therefore the tensile stress formed by the cooling of the weld zone gives rise to compressive stresses on either side of the weld center line.

The magnitude of residual stresses recorded for both insulated and non-insulated pipe coupons were different. Case 2 recorded a peak tensile stress of 540 MPa when cooled without insulation and 490 MPa when cooled with the insulator. Case 3 had a peak tensile stress of 525 MPa when cooled without the insulator and 360 MPa when cooled with the insulator. Case 4 had a peak tensile stress of 340 MPa when cooled without the insulator and 250 Mpa when cooled with the insulator. There was a reduction in the maximum axial tensile residual stresses on the inner side of the pipe when the insulator was used. For instance, axial tensile residual stresses on the inner surface of the pipe were lowered by 31.4 percent when 25 mm thick insulation was used.

Low cooling rates cause a reduction in residual stresses in samples [48, 49]. The change in cooling rate also changes the distribution of residual stresses [48].

There are three primary causes for residual stresses namely: Thermal variation, phase transformation, and mechanical processing. Residual stresses caused by

thermal variation are due to the difference in the cooling rate throughout the body when it is heated to a very high temperature. During welding, the weld zone is heated to temperatures above the melting point of the base metal. Therefore, during cooling the weld-zone will have a higher cooling rate compared to the base metal. The difference in cooling rates results in localized variations in thermal contraction. Hence non-uniform stresses develop. Contraction at the weld zone is restricted by the base metal giving rise to tensile residual stresses. The cooling rate therefore plays a major role in setting up residual stresses in welded parts. Rapid cooling of a part from high temperature causes large thermal gradients and hence large thermal stresses. Lowering the cooling rate, e.g., by insulation tends to ensure uniform cooling rate of the metal and hence decreased tensile residual stresses.

Reduction of tensile residual stress is beneficial to any engineering structure. Tensile residual stresses are known to facilitate harmful processes such as SCC, corrosion fatigue, etc. In pipelines, a slow cooling rate helps to reduce residual stresses by ensuring the inside and outside of the pipe cool at about the same rate.

4.3.1.2 Axial Stress Distribution for the Outer Pipe Surfaces

Figures 18-20 show axial residual stress distribution on the outer section of the pipe.

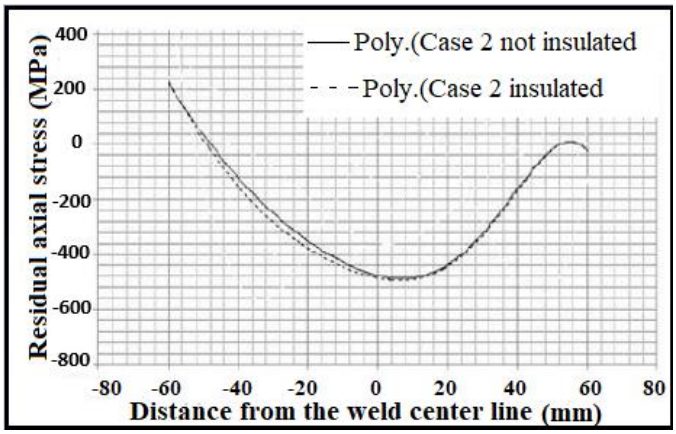

Fig. 18. Simulated axial stress distribution for the outer pipe surfaces for case 2.

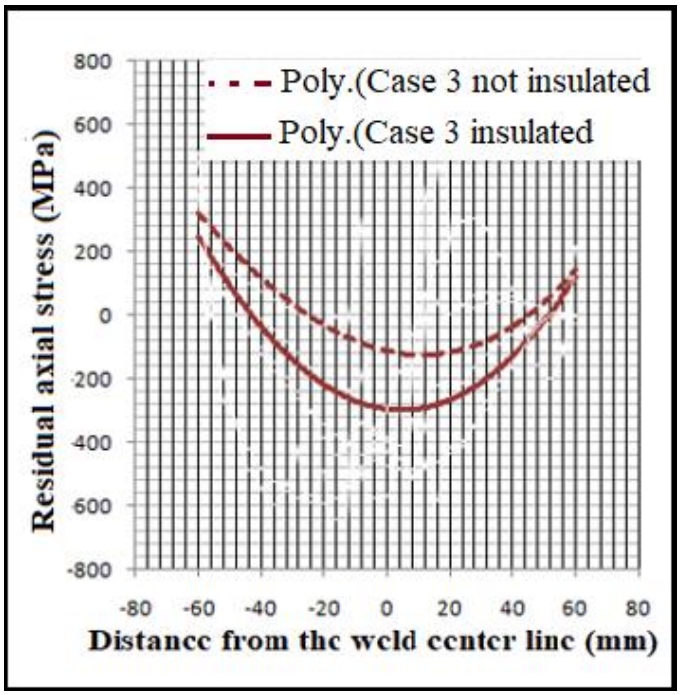

Fig. 19. Simulated axial stress distribution for the outer pipe surfaces for case 3.

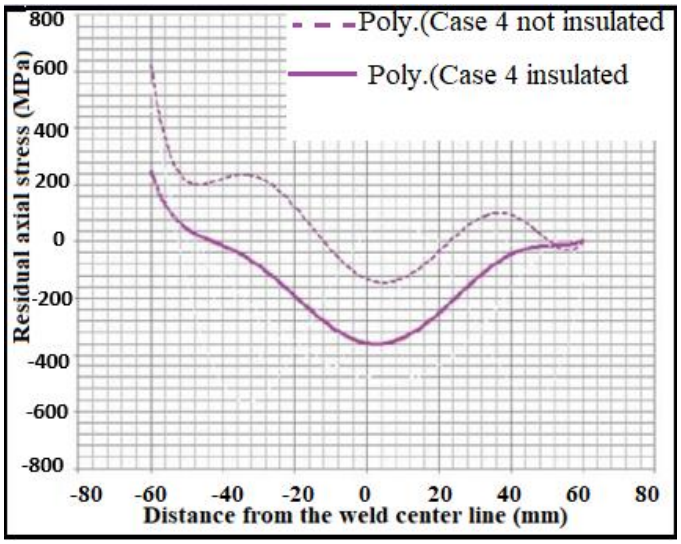

Fig. 20. Simulated axial stress distribution for the outer pipe surfaces for case 4.

Figures 18-20 show the residual stress distribution for the pipe coupons that were covered with insulators of thicknesses 12.5 mm, 25 mm, and 37.5 mm respectively. Generally, it is observed from the graphs that the stresses are compressive along the weld center line and tensile away from the weld center line. This residual stress distribution was also observed by other researchers [46, 47].

As stated earlier, residual stresses are self-equilibrating in nature. Since the inner side already has tensile stresses, it follows that the stresses in the outer section will be compressive in nature in an attempt to create a stable state of equilibrium. The outer surface

was also welded last and hence last to cool. As a rule of thumb in the study of residual stresses, areas that cool down last induce compressive stresses in formerly cooled areas [22]. Hence compressive residual stresses are developed along the weld-zone on the outer surface of the pipe because it cools last.

From the graphs in Figures 18 - 20, case 2 had a maximum compressive stress of 520 MPa for the pipe that cooled with insulation and 518 MPa for the case that cooled without insulation. Case 3 had a maximum compressive stress of 290 MPa for the pipe that cooled with insulation and 120 MPa for the case that cooled without insulation. Case 4 had a compressive stress of 360 MPa when cooled with insulation and 130 Mpa for the case that was cooled without insulation. Axial compressive residual stresses on the outer surface of the pipe increased by 176.9 percent when 37.5 mm thick insulation was used. This indicates that insulating the pipe after welding produced larger axial compressive stresses for the insulated pipe coupons.

Higher residual compressive stresses were developed for the cases that were insulated compared to those that cooled without insulation. Following the general principle applied to the study of residual stresses in welded steel, i.e., the area of the body that hardens last is in residual compression [22]. We can deduce that if two metals were to be cooled separately the metal that would take longer to cool would develop larger compressive stresses as was the case in this research.

It was observed that after welding, the time it took before covering the coupons with the insulator had a significant impact on how effective the insulation was. A large delay time before lagging could render the insulation ineffective. In such a case, the residual stresses obtained were almost equal in magnitude to the residual stresses set up when the weldment cooled in air. As was the case in Fig. 18 in which there was a larger delay time before the application of insulator on the outer section of the pipe.

In general, compressive residual stress at the surface of a component is beneficial: it tends to increase fatigue strength and fatigue life, slow crack propagation, and increase resistance to environmentally assisted cracking, such as stress corrosion cracking and hydrogen-induced cracking.

5. Conclusion

Based on the outcome of this research, the following conclusions were made:

a) Insulating reduced tensile residual stresses of welded structure on the inner surface of the pipe.
b) Insulating also increases compressive residual stresses on the outer surface of the pipe.
c) Insulating to lower cooling rate is a beneficial and practical approach that can be used to improve the integrity of a welded pipe.

References

[1] A. Ghani, "Residual Stresses and Heat Treatments for Metallic Welded Components" PhD thesis, Dublin City University, School of Mechanical and Manufacturing Engineering, 1994.

[2] T. Pharris1 and R Kolpa, “Overview of the Design, Construction, and Operation of Interstate Liquid Petroleum Pipelines,” tech. rep., 2007. Technical Report.

[3] E. Menon, “Transmission Pipeline Calculations and Simulations Manual”, Book published by Elsevier, 2015.

[4] D. Furchtgott-Roth, “Pipelines are Safest for Transportation of Oil and Gas”, Issue Brief No. 23, June 2013, Manhattan Institute for Policy Research.

[5] P. Hopkins, “ High Design Factor Pipelines: Integrity Issues”, The Journal of Pipeline Integrity, pg. 69–97, 2005.

[6] R. Revie, “Oil and Gas Pipelines, Integrity and Safety Handbook”, John Wiley and Sons, Hoboken, New Jersey, 2015.

[7] H. Rampaul, “Pipe Welding Procedures”: Second Edition. Book by Industrial Press, New York, 2003.

[8] R. Messler, “Principles Of Welding: Processes, Physics, Chemistry, and Metallurgy”, Book by Wiley Publisher: Second Edition, 2004.

[9] “Welding Techniques used for pipes”, The Pipingmart, Industrial manual, 2022

[10] G. Antaki, “Piping and Pipeline Engineering Design, Construction, Maintenance, Integrity, and Repair”: First Edition. Book by Marcel Dekker, Inc., 2003.

[11] Mechanical Engineering Resources, “Codes and Standards”, 2022. Industrial Manual.

[12] International Standards, ISO 13623: “Petroleum and Natural Gas Industries-Pipeline Transportation Systems”, 2021. Industrial Manual

[13] American Society of Mechanical Engineers (ASME), ASME B31.8: “Gas Transmission Distribution Piping Systems”, 2021. Industrial Manual

[14] British Standards Institution (BSI), “PD 8010 Pipeline Systems Steel pipelines on Land. Code of practice”, 2022. Industrial Manual.

[15] H. Rampaul, “Pipe Welding Procedures”, Second Edition Book by Industrial Press, Newyork, 2003.

[16] M. Qureshi, “Analysis Of Residual Stresses and Distortions In Circumferentially Welded Thin-Walled Cylinders”. PhD thesis, National University of Sciences and Technology, School of Mechanical and Manufacturing Engineering, 2008.

[17] G. Schajer, “Practical Residual Stress Measurement Methods”. Book by John Wiley & Sons Publishers, 2013

[18] M. Yu, “Unified Strength Theory and Its Applications”, vol. 10. Book Published by Springer: Second Edition, 2019.

[19] Miller Welds, “Guidelines for Pipe Welding”, 2018. Industrial Manual.

[20] American Petroleum Institute (API), API RP 1111: “Design, Construction, Operation, and Maintenance of Offshore Hydrocarbon Pipelines”, 2021. Industrial Manual

[21] K. Kesavan, K. Ravisankar, S. Parivallal, P. Sreeshylam, “Non-destructive evaluation of residual stresses in welded plates using the barkhausen noise technique, Experimental Techniques Research Journal, vol. 29, no. 5, pp. 17-21, 2005.

[22] D. Wulpi, “Understanding How Components Fail”, Book published by ASM International, 2nd edition, 1999.

[23] P. Michaleris, “Minimization of welding distortion and buckling Modelling and implementation” Book published by Woodhead publishers, pp 3-20, 2011.

[24] Vishay Precision Group, “Measurement of Residual Stresses by the Hole-drilling Strain Gage Method”, 2010. Industrial Manual.

[25] D. Radaj, "Heat Effects of Welding Temperature Field, Residual Stress, Distortion", Book published by Springer-Verlag Berlin Heidelberg, 1992.

[26] A.Niku-lari, "Advances In Surface Treatments Technology-Applications-Effects" Published by Pergamon Press, 1987.

[27] M. Hussain, T Zhang, S Khan, N Hassan, "Stress Corrosion Cracking Is A Threat To Pipeline Integrity Management", conference paper, 2020

[28] Y. Shi, B. Chen and J. Zhang, "Effects of welding residual stresses on fatigue crack growth behavior in butt welds of a pipeline steel", Engineering Fracture Mechanics, vol. 36, no. 6, pp. 893-902, 1990.

[29] Z. Feng, "Processes and Mechanisms of Welding Residual Stress and Distortion" Woodhead Publishing Limited, England, 2005

[30] Hobart Brothers, "Understanding Weld Cracking", 2009. Industrial Manual

[31] Maine Welding Company, "Welding Stresses and Cracking", 2018. Industrial Manual.

[32] A. Mirzaee and G. Wu, "Residual stress in pipeline girth welds-a review of recent data and modeling", International Journal of Pressure Vessels and Piping, vol. 169, pp. 142-152, 2019.

[33] D. Kollar, B. kovesdi and J. Nezo, "Numerical simulation of welding process-application in buckling analysis", Periodica Polytechnica Research Journal, vol. 61, no. 1, pp. 98-109, 2017.

[34] Z. Samad, N. Nor and E. Fauzi, "Thermo-Mechanical Simulation of Temperature Distribution and Prediction of Heat-Affected Zone Size in MIG Welding Process on Aluminium Alloy EN AW 6082-T6", IOP Conference Series: Materials Science and Engineering, vol. 530, pp. 1-15, 2019.

[35] J. Hanse, "Numerical Modeling of Welding Induced Stresses". PhD thesis, Technical University of Denmark: Department of Manufacturing Engineering and Management, 2003.

[36] A. Robertson and J. Svedman, "Welding simulation of a gear wheel using FEM", Masters Thesis: Chalmers University of Technology: Department of Materials and Manufacturing Technology, 2013

[37] W. Zhang, J. Gunnars, P. Dong and J. Hong, "Improvement and validation of weld residual stress modeling procedure", 2009. Technical Report.

[38] A. Lundbäck, "Modelling and Simulation of Welding and Metal deposition". PhD thesis, Luleå University of Technology, Department of Applied Physics and Mechanical Engineering: Division of Computer Aided Design, 2010.

[39] E.G. Ovy, "Comparison between 4 and 8 Node Integration Elements in Finite Element Analysis " June 2020, technical report

[40] S. Adeeb, "Introduction to solid mechanics: Finite element analysis" Engineering at Alberta, 2020

[41] Simulia, "ABAQUS user manual" Dassault Systemes, 2020

[42] H. Coules, "Contemporary approaches to reducing weld induced residual stress" Materials science and technology, Journal Published By Maney Publishing, vol. 29, no. 1, pp. 4-18, 2013.

[43] A. Yaghi, T. Hyde, A. Becker, J. Williams and W. Sun, "Residual Stress Simulation in Welded Sections of P91 Pipes", Journal of Materials Processing Technology, vol. 167, no. 2, pp. 480-487, 2005.

[44] A. Yaghi, D. Tanner, T. Hyde, A. Becker and W. Sun, "Finite Element Thermal Analysis of the Fusion Welding of a P92 steel pipe", Mechanical Sciences, vol. 3, no. 1, pp. 33-42, 2012.

[45] Advanced Materials Testing: Netsch, "Thermal Insulation Materials", 2020. Industrial Manual.

[46] D. Akbari, M. Farahani and N. Soltani, "Effects of the weld groove shape and geometry on residual stresses in dissimilar butt-welded pipes", Journal of Strain Analysis, vol. 47, no. 2, pp. 73-82, 2012.

[47] M. Peric, I. Garasic, N. Gubeljak, Z. Tonkovic, S. Nizetic and K.Osman, "Numerical Simulation and Experimental Measurement of Residual Stresses in a Thick-Walled Buried-Arc Welded Pipe Structure", Metallurgy Journal, vol. 12, no. 7, pp. 277-281, 2022.

[48] Y. Zhang, Y. Yi, S. Huang and F. Dong, "Influence of Quenching Cooling Rate on Residual Stress and Tensile Properties of 2A14 Aluminum Alloy Forgings", Materials Science and Engineering: Elsevier Journal, vol. 674, pp. 658-665, 2016.

[49] Z. Zhang, W. Wang, H. Fu and J. Xie, "Effect of Quench Cooling Rate on Residual Stress, Microstructure and Mechanical Property of an Fe-6.5Si Alloy", Materials Science and Engineering A: Elsevier Journal, vol. 530, pp. 519-524, 2011.